Low-Temperature Oxidation Characteristics of Lignite Chars from Low-Temperature Pyrolysis

ARTICLE *in* ENERGY & FUELS · AUGUST 2014

Impact Factor: 2.79 · DOI: 10.1021/ef501004t

7 AUTHORS, INCLUDING:

Arash Tahmasebi
University of Science and Technology Liaoning
36 PUBLICATIONS **397** CITATIONS
SEE PROFILE

T. F. Wall
University of Newcastle
191 PUBLICATIONS **5,253** CITATIONS
SEE PROFILE

energy&fuels

Article

pubs.acs.org/EF

Low-Temperature Oxidation Characteristics of Lignite Chars from Low-Temperature Pyrolysis

Fanrui Meng,[†] Arash Tahmasebi,[†] Jianglong Yu,*[,†,‡] Huan Zhao,[§] Yanna Han,[†] John Lucas,[‡] and Terry Wall[‡]

[†]Key Laboratory of Advanced Coal and Coking Technology of Liaoning Province, School of Chemical Engineering, University of Science and Technology Liaoning, Anshan, Liaoning 114051, People's Republic of China

[‡]Chemical Engineering, University of Newcastle, Callaghan, New South Wales 2308, Australia

[§]Thermal Energy Research Centre, Shenyang Aerospace University, Shenyang, Shenbei 110136, People's Republic of China

ABSTRACT: The oxidation characteristics of chars from low-temperature pyrolysis of two lignite coals have been systematically investigated using a dual fixed-bed quartz reactor and a thermogravimetric analyzer (TGA). During oxidation experiments, the temperature profiles of coal and char samples were recorded and CO_2 and CO gases evolved were analyzed using gas chromatography. The physical and chemical structures of coals and chars were analyzed using Brunauer−Emmett−Teller (BET) adsorption isotherms and Fourier transform infrared spectroscopy (FTIR). During oxidation, the temperature of the coal sample may increase noticeably, exceeding the crossing point temperature (CPT). Chars prepared at 400 °C showed the lowest CPT, indicating the highest oxidation reactivity compared to that of parent coals and chars prepared at other temperatures. During oxidation, gaseous products are released, implying that oxygen-containing functional groups and solid oxygenated complexes decomposed and the yields increased with increasing the oxidation temperature. The amount of CO_2 generation was proportional to that of CO with the molar ratio of CO_2/CO at around 4.15 under the present experimental conditions. During non-isothermal oxidation, the concentration of OH and other oxygen-containing functional groups increased with increasing the oxidation temperature for char samples but decreased in the case of oxidized coal. During isothermal oxidation, the concentration of oxygen functional groups in coal decreased with increasing the oxidation temperature above 250 °C. Pre-oxidation of chars decreased their combustion reactivity measured on the TGA.

1. INTRODUCTION

Low-rank coals account for approximately half of the global coal resources[1] and are playing an increasingly important role in supplying primary energy in developing countries, such as China. Low-rank coals have some advantages over higher rank coals, such as low mining cost, high reactivity, high amount of volatiles, and low pollution-forming impurities, such as sulfur, nitrogen, and heavy metals.[1] However, the high moisture content and low calorific value in low-rank coals significantly limits their application. During transportation and storage, low-rank coals tend to spontaneously combust, mainly as a result of low-temperature oxidation.

Low-temperature oxidation characteristics of coal have been extensively reported in the literature.[2−7] Lu et al.[2] studied the oxidation and pyrogenation of a Chinese lignite below 150 °C by thermal analysis. Their results showed that low-temperature oxidation is clearly an exothermic process contrasted with the pyrogenation process. Qi et al.[3] reported that the correlation of oxygen consumption with temperature is nonliner and is closely related to coal rank. Khan[5] found that the hydrogen contents in chars correlated well with its reactivity and the oxygen chemisorption capacity is the determining parameter for char reactivity. Clemens et al.[4] investigated the role of moisture in self-heating of low-rank coals. Their results showed that moisture favors the formation of radical sites. They also reported that low-rank coals with 5−10 wt % moisture content undergo oxidation more rapidly than completely dried coal. Wang et al.[6] analyzed the thermal decomposition of solid oxygenated complexes formed by coal oxidation at low temperatures. Their results showed that the rates of CO_2 and CO evolution were dependent upon the temperature but independent of the coal particle size. Yürüm et al.[8] reported that, with increasing time and oxidation temperature, the intensity of aromatic C═O groups increased significantly, while that of aliphatic C−H groups decreased. Studies on other aspects of coal oxidation at low temperatures have also been studied in the literature.[7−13]

Low-temperature pyrolysis is regarded as an effective way to upgrade low-rank coals, such as lignite.[14,15] Chars from low-temperature pyrolysis of lignite may be used as a fuel for power generation, to substitute thermal coals or pulverized coal injection (PCI) coals in combustion or as inert components in blends for coke making.[16] During the pyrolysis process, sulfur and nitrogen would be released as sulfur and nitrogen compounds, such as H_2S, COS, and NO_x precursors, such as NH_3 and HCN. Therefore, less sulfur and nitrogen will be retained in char, which will, in turn, decrease the emissions of sulfur and NO_x during char combustion. However, during handling, storage, and transport, these chars may undergo low-temperature oxidation and, subsequently, spontaneous combustion, causing serious safety problems. In our previous study, it was observed that physical and chemical structures of chars from low-temperature pyrolysis changed with the temperature,[16] which further significantly affected char reactivity during combustion and low-temperature oxidation.

In comparison to coal oxidation, char oxidation at a low temperature is less studied. A general description of char oxidation is

Received: May 3, 2014
Revised: July 15, 2014
Published: August 7, 2014

given in the literature. Char oxidation takes place in several steps,[5,17] i.e., diffusion of oxygen to reactive sites (including bulk diffusion and internal diffusion), chemisorption of oxygen on the surface of carbon (active sites), surface reaction of chemisorbed oxygen with carbon to form oxidation products, desorption of oxidation products from the carbon surface, and diffusion (mass transfer) of oxidation products from the carbon surface to the char particle surface and bulk phase. The new active sites at the carbon surface are generated during the evolution of volatile matter in coal.[3] The concentration of these active sites in char determines its reactivity during oxidation. Chars from low-temperature pyrolysis of lignite are prone to low-temperature oxidation and spontaneous combustion. The low-temperature oxidation of char is affected by the degree of physical and chemical structure changes during the pyrolysis process.

Chars from low-temperature pyrolysis of lignite behave differently during low-temperature oxidation compared to their parent coals. A full understanding of the exact mechanism of low-temperature oxidation of chars is not yet achieved. The objective of this study is to investigate the low-temperature oxidation characteristics of chars from two lignite coals using a dual fixed-bed quartz reactor, thermogravimetric analyzer (TGA), and differential scanning calorimeter (DSC). The evolution of gaseous products during oxidation and the effects of changes in functional groups during pyrolysis on char oxidation reactivity at low temperatures were studied in detail.

2. EXPERIMENTAL SECTION

2.1. Sample Preparation. Two lignite coals, a Chinese lignite from the Inner Mongolia region (HL) and an Indonesian lignite (YN), were used in this study. The proximate and ultimate analyses of these coals are given in Table 1. The raw coal samples were crushed and sieved to less than 0.2 mm. To produce chars, about 2 g of coal was heated in a tubular quartz reactor in an electric furnace in nitrogen gas with a flow rate of 200 mL/min for 30 min. The pyrolysis was carried out at 400 and 550 °C.

Table 1. Proximate and Ultimate Analyses of Raw Coal Samples

coal sample[a]	HL	YN
moisture content (wt %, ad)	14.88	20.38
volatile matter (wt %, ad)	33.98	38.87
ash (wt %, ad)	12.12	6.02
fixed carbon (wt %, ad)	39.02	34.73
C (wt %, db)	61.99	69.3
H (wt %, db)	5.05	4.79
N (wt %, db)	0.8	1.0
S (wt %, db)	0.26	0.24
O (by difference) (wt %, db)	19.78	18.65

[a]ad, air-dried; db, dry basis.

2.2. Oxidation Experiments. The isothermal oxidation experiments of coal and char samples were carried out in a fixed-bed quartz reactor heated in an electric furnace in air at a flow rate of 400 mL/min for 8 h. Details of the experimental setup used for isothermal oxidation are reported elsewhere.[16] Briefly, 2.0 g of the samples was used for each oxidation experiment. When the furnace was heated to the desired oxidation temperatures (50, 150, 250, and 300 °C), the reactor loaded with coal samples was placed into the furnace and heated for 8 h. All of the experimental runs were repeated 3 times, and the results reported here are the averages of three measurements, with the experimental error ranging between ±6% of the mean value.

Non-isothermal oxidation experiments were carried out in both TGA and dual fixed-bed reactors. The TGA (NETZSCH STA 449 F3) was used to carry out the TGA non-isothermal oxidation of coal and char. Samples of 15.0 mg were placed into a platinum crucible and heated at a heating rate of 3 °C/min from 30 to 310 °C under air at 100 mL/min flow rate. Prior to TGA analysis, coal samples were dried at 105 °C for 2 h. The main difference between TGA experiments and those carried out in a fixed-bed quartz reactor was the mode of heating. TGA and fixed-bed

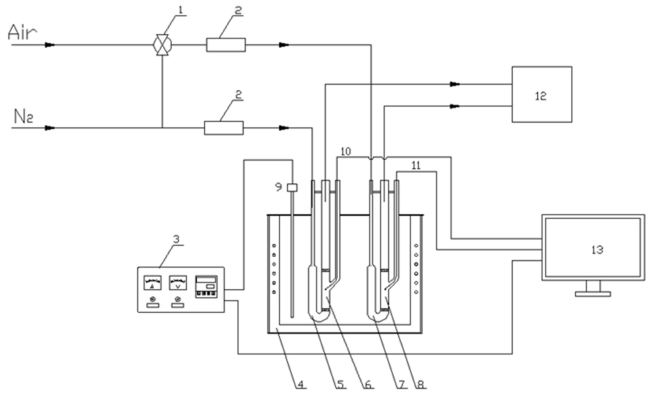

Figure 1. Schematic diagram of the dual fixed-bed reactor experimental setup for coal and char oxidation: (1) bypass valve, (2) mass flow controller, (3) temperature controller, (4) furnace, (5 and 7) quartz reactor, (6 and 8) coal/char sample, (9–11) thermocouples, (12) gas chromatography, and (13) data acquisition unit.

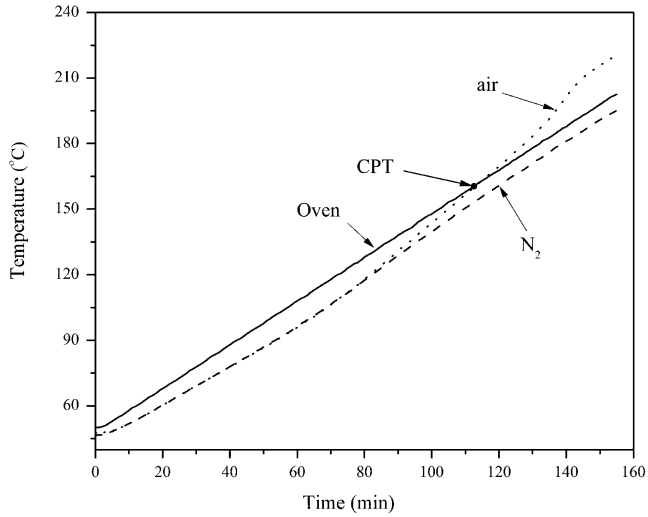

Figure 2. Definition of the CPT during dual fixed-bed reactor oxidation.

Table 2. Band Positions and Assignments in the FTIR Spectra of Lignite Samples

position (cm^{-1})	assignment	position (cm^{-1})	assignment
3610	free OH groups	1500	aromatic C═C
3516	OH–π hydrogen bonds	1458	asymmetric CH_3– and CH_2–
3400	self-associated OH	1437	aromatic C═C
3300	OH–ether O hydrogen bonds	1410	asymmetric CH– (CH_3) and OH
3200	tightly bound cyclic OH tetramers	1377	symmetric CH_3–Ar and R
3050	aromatic hydrogen	1350	symmetric CH_2–C═O
1772	aryl esters	1274	C–O in aryl ethers
1703	carboxyl acids	1222	C–O, OH, phenoxy structures, and ethers
1650	conjugated C═O	1168	C–O phenols and ethers
1610	aromatic C═C	1094	C–O secondary alcohols
1586	aromatic C═C	1036	alkyl ethers

dx.doi.org/10.1021/ef501004t | Energy Fuels 2014, 28, 5612–5622

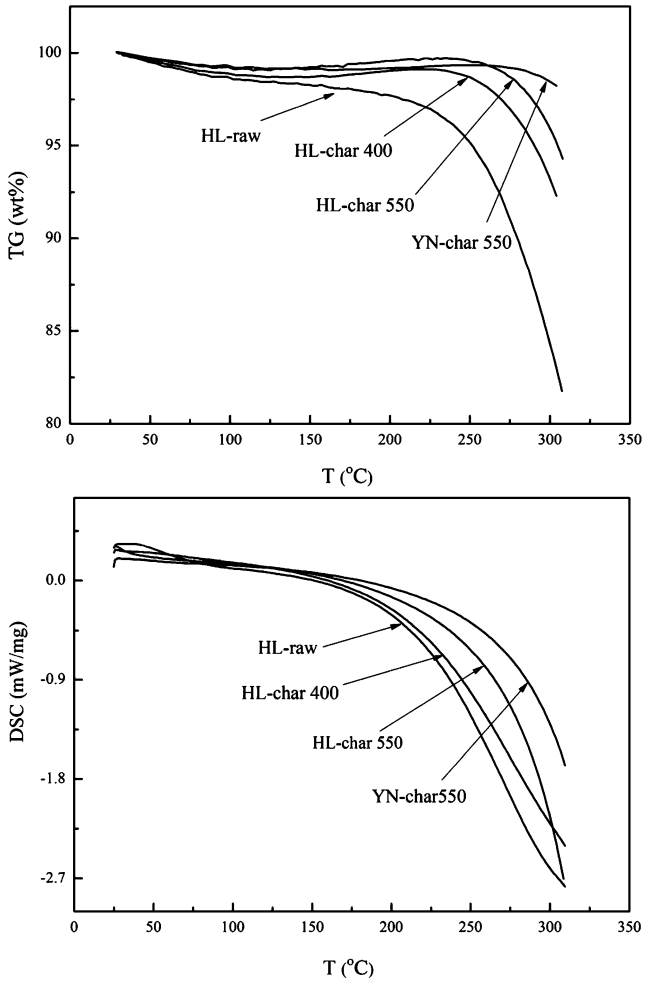

Figure 3. Thermogravimetry (TG) and DSC curves of low-temperature oxidation of coal and char samples.

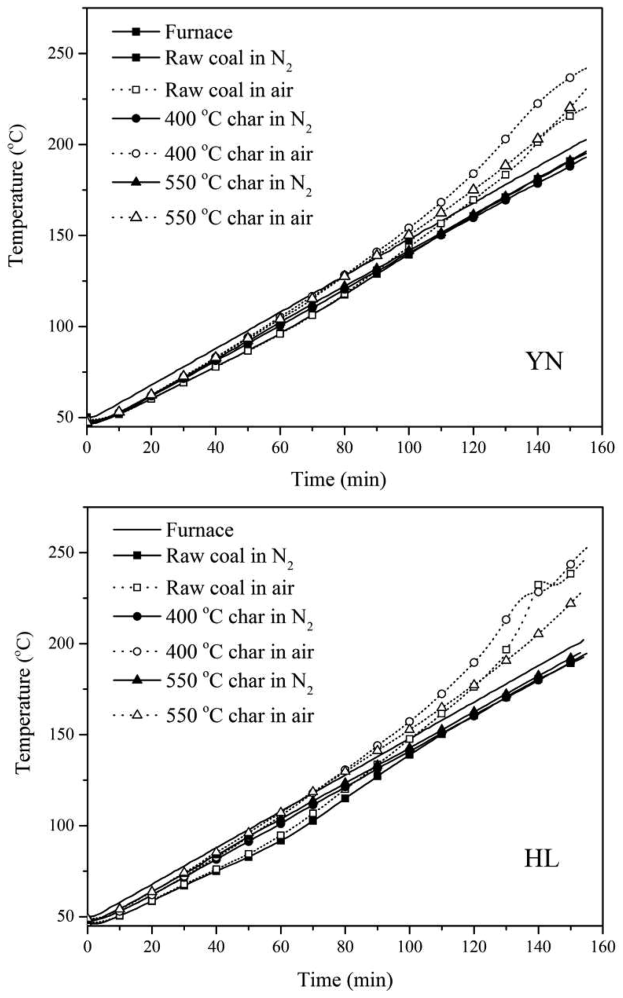

Figure 4. Thermograms for oxidation of raw coals and chars (heating rate, 1 °C/min; sample weight, 6 g; and N_2 flow rate, 30 mL/min).

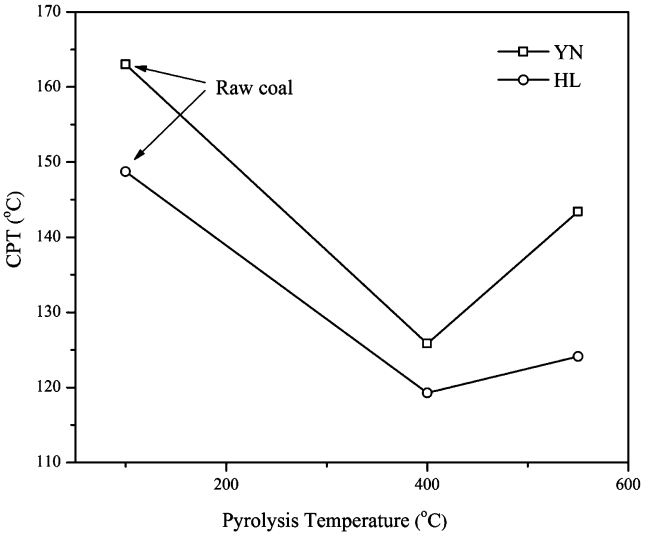

Figure 5. Changes in CPT of YN and HL raw coals and chars.

experiments were carried out in non-isothermal and isothermal modes, respectively. The thermal analysis of coal and char samples was carried out using a DSC (NETZSCH DSC 200 F3). Samples of 5.0 mg were placed in an aluminum pan and heated at a heating rate of 3 °C/min from 30 to 310 °C under air with 100 mL/min flow rate.

Fixed-bed non-isothermal experiments were carried out in an experimental setup shown in Figure 1. The oxidation experiments were carried out in a dual fixed-bed quartz reactor with an inner diameter of 20 mm heated in an electric furnace (SY60, Shenyang General Furnace Manufacturing Co., Ltd., China). Before each experiment, 6 g of sample was placed into the two reactors. Temperatures of the furnace and the coal sample were measured using two thermocouples. As soon as these temperatures became the same, the carrier gas in the oxidation reactor was switched to air of the same flow rate to start the low-temperature oxidation experiment. The furnace was heated from 50 to 200 °C at the rate of 1 °C/min. Coal bed temperatures during the heating process under both air and nitrogen were recorded by thermocouples, and the data were transferred to the computer through a data acquisition system (Advantech USB-4718, Taiwan). The concentrations of CO_2 and CO at the reactor exit were measured using gas chromatography (G5, Beijing Puxi General Instrument Co., Ltd., China) equipped with a flame ionization detector (FID). The evolution rates of CO and CO_2 were calculated from the following equations:[6,18,19]

$$R_{CO_2} = \frac{C_{CO_2}}{W} V_{gas} \quad (1)$$

$$R_{CO} = \frac{C_{CO}}{W} V_{gas} \quad (2)$$

where C_{CO_2} and C_{CO} are carbon dioxide and carbon monoxide concentrations at the reactor exit, respectively. V_{gas} is the volumetric flow rate of the carrier gas, and W is the dry mass of the coal sample.

The crossing point temperature (CPT), as shown in Figure 2, is defined as the point at which the coal temperature exceeds the furnace

dx.doi.org/10.1021/ef501004t | Energy Fuels 2014, 28, 5612−5622

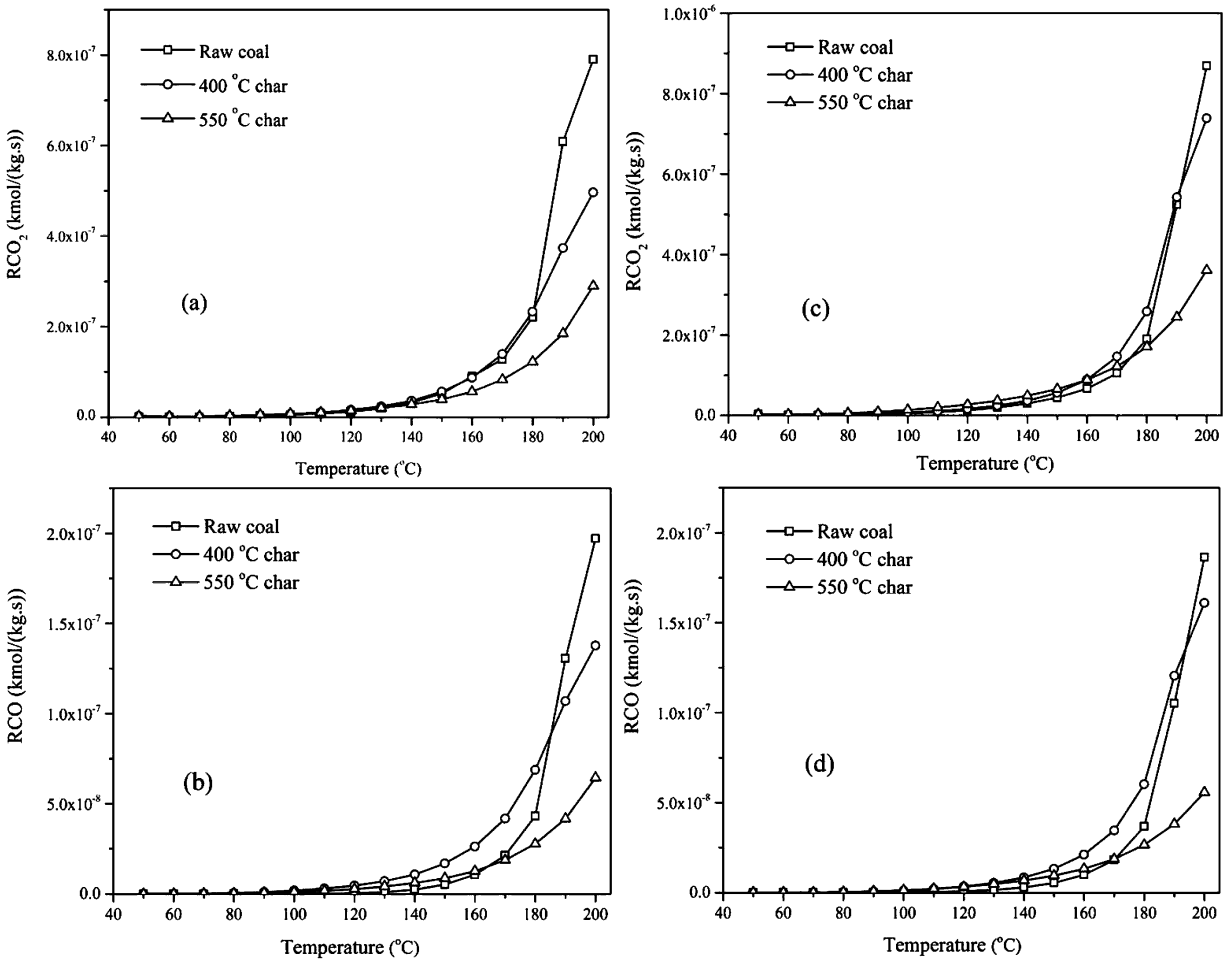

Figure 6. Rates of CO_2 and CO evolution during heating of raw coals and chars as a function of the oxidation time: (a and b) YN and (c and d) HL.

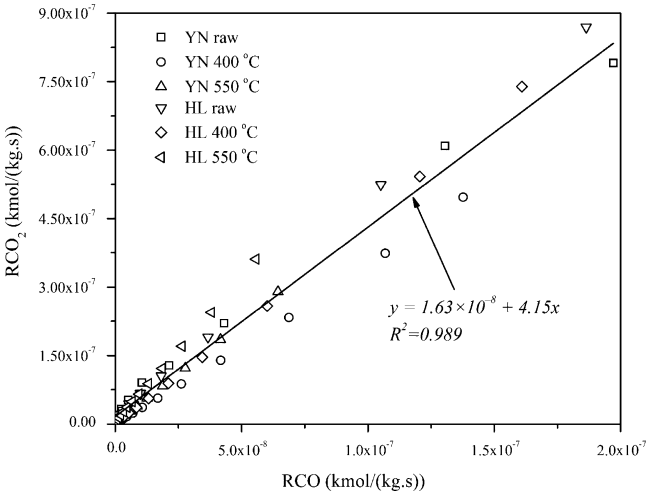

Figure 7. Correlations between the evolution rate of CO_2 and CO.

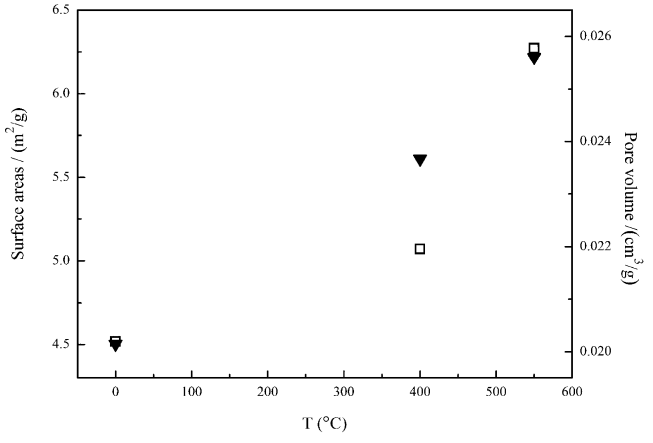

Figure 8. Surface areas and pore volume of HL coal and its char samples: (□) surface areas and (▼) pore volume.

temperature and is considered as the point of ignition. This point is an indicator of the propensity of a coal to spontaneously combust.[20]

2.3. Char Characterization. The surface area and porosity of coal and char samples were measured with a specific surface area and pore size analyzer (V-sorb 4800 P). Nitrogen was used as the adsorption gas at 77 K. Samples were dried at 105 °C and then degassed in the adsorption system at 200 °C to a final pressure of 1.33×10^{-4} Pa for 4 h. To ensure the reproducibility and accuracy of data, the measurements were repeated 3 times, and their average is reported here. The Barrett–Joyner–Halenda (BJH) model was used to determine the pore size distributions from the desorption isotherm.[21−23]

Infrared (IR) spectra of the coal and char samples were obtained using a FTIR spectrometer (Thermo Scientific Nicolet IS5). Calibration of the FTIR spectrometer was carried out using the internal calibration source as well as a mid-IR diffuse reflectance wavelength standard. Prior to FTIR measurements, a reference spectrum was obtained from pure KBr pellets without the addition of any coal or char sample. The background reference spectrum was subtracted from subsequent measurements. Pellets were prepared by grinding 1 mg of sample with

dx.doi.org/10.1021/ef501004t | Energy Fuels 2014, 28, 5612−5622

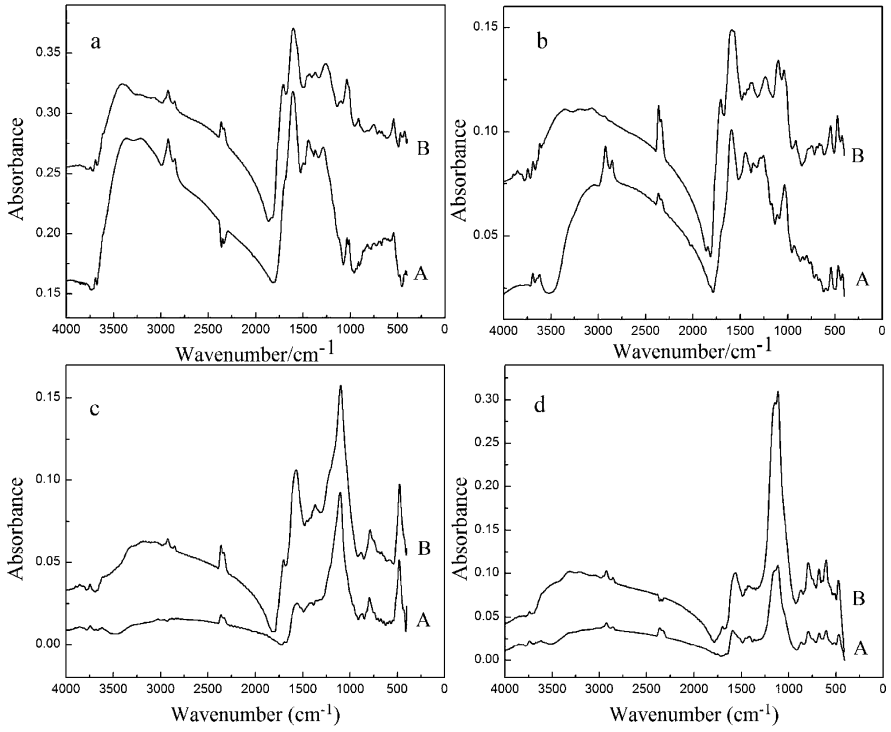

Figure 9. FTIR spectra of (A) raw coal or char samples in comparison to (B) samples after non-isothermal oxidation: (a) HL raw coal, (b) HL char at 400 °C, (c) HL char at 550 °C, and (d) YN char at 550 °C.

120 mg of KBr. IR spectra of the coal and char samples in the oxygen-containing functional groups regions were resolved by curve-fitting analysis[24−28] using a commercially available data-processing program (OriginPro, OriginLab Corporation). The assignment of the bands in the IR spectra (Table 2) was made according to the literature.[24,27,29−34] Prior to curve-fitting analysis, the mineral matter corrections were applied on IR spectra.[35−37] HL and YN ash samples were obtained at 500 °C. The IR spectra of ash samples were subtracted from the corresponding coal and char samples, and the ash-free IR spectra of samples were further analyzed by curve-fitting analysis. The Gaussian function was used as the mathematical function, and the coefficient of determination (COD) was the primary criterion in examining the goodness of curve fitting.[16,27] COD values of the curve-fitting analysis in all cases were above 0.999, indicating that IR spectra of all samples were curve-fitted with high accuracy.

3. RESULTS AND DISCUSSION

3.1. Non-isothermal Oxidation in TGA and DSC. As shown in Figure 3, the TGA and DSC curves revealed significant differences in oxidation behavior of raw coal and char samples. As expected, the total mass loss up to 310 °C for HL raw coal was greater than that of HL chars. The DSC results show that the exothermic peaks of coal and chars are consistent with the mass loss curves. The temperature corresponding to the initial oxidation was lower for raw coal compared to chars. In the case of chars, the temperature corresponding to the initial oxidation increased with increasing the pyrolysis temperature.

3.2. Fixed-Bed Non-isothermal Oxidation. Figure 4 shows the temperature profiles of the furnace and sample bed in air and nitrogen. For each sample, changes in temperatures of two coal samples with linearly increasing the furnace temperature were divided into three stages: (a) the initial stage during which the two temperatures in air and nitrogen were the same and increased monotonically, (b) the oxidation stage during which the two temperatures increased at different rates, and (c) the self-heating stage during which the temperature of the coal sample in air exceeded the furnace temperature. The CPT for YN and HL coals and their low-temperature chars are shown in Figure 5. The temperature of the coal sample increased to above the CPT because of exothermic oxidation reactions. A higher rate of temperature rise for samples in air compared to that in nitrogen implies the high propensity of the char sample to self-heating and spontaneous combustion. Chars prepared at 400 °C showed the lowest CPT, suggesting the highest oxidation reactivity of these chars compared to corresponding raw coals and chars prepared at 550 °C. Our previous study also showed that chars prepared at low temperatures (400−450 °C) had higher combustion reactivity compared to their parent coals and higher temperature chars.[16]

The evolution of the gases produced during oxidation was studied by gas chromatography and is shown in Figure 6. Main gases evolved were CO and CO_2, together with negligible amounts of H_2O. In this study, the concentrations of CO and CO_2 were measured to investigate the mechanism of oxidation. With increasing the furnace temperature, the evolution rates of CO_2 and CO for all samples increased monotonically up to 130 min and increased markedly thereafter. The release of a larger number of gaseous products implied that oxygen-containing functional groups and solid oxygenated complexes decomposed with increasing the oxidation temperature.[38] During oxidation, the rate of CO_2 production significantly exceeded that of CO in all samples. Similar results have been reported in the literature.[6,38,39] The production rate of gaseous products was lowest for chars prepared at 550 °C probably because of the loss of active sites on the char surface during pyrolysis. The relationship between the gaseous oxidation products is shown in Figure 7. It can be seen that the amount of CO_2 generation was proportional to that of CO. The ratio of CO_2/CO production was independent of experimental conditions

dx.doi.org/10.1021/ef501004t | Energy Fuels 2014, 28, 5612−5622

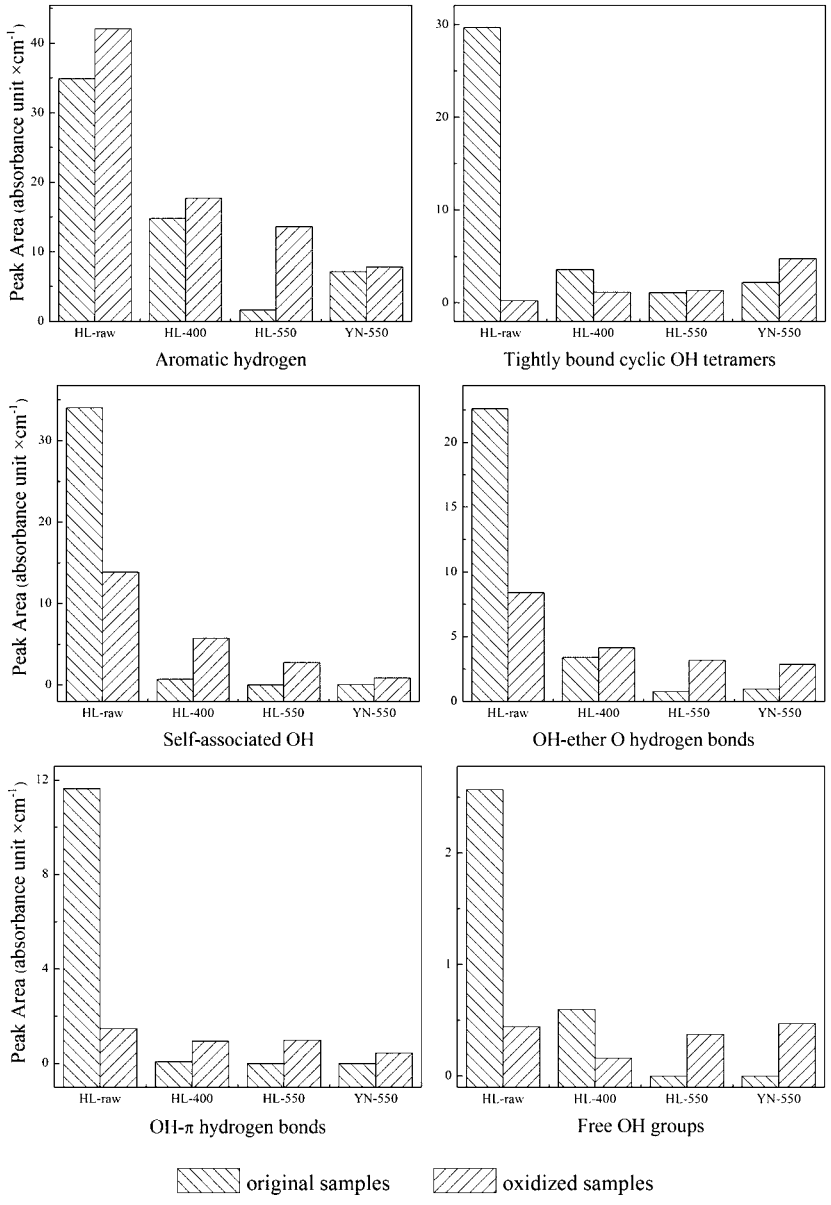

Figure 10. Changes in OH group absorption during non-isothermal oxidation of coal and char samples.

and type of samples used. The molar ratio of CO_2/CO production was approximately 4.15 under present experimental conditions. This value was similar to those reported in the literature.[39]

3.3. Surface Areas and Pore Structure. Char surface areas and pore volume increased with increasing the pyrolysis temperature, as shown in Figure 8. The changes in the pore structure and specific surface areas of coal can affect the reactivity of char during gasification or combustion. The increased specific surface areas and porosity can increase the char oxidation reactivity.[3,40] However, it was observed that the oxidation reactivity of char samples prepared at 550 °C was lower compared to that of raw coal and 400 °C chars (Figure 5). This suggested that factors other than surface area and porosity are having a greater influence on oxidation reactivity of chars obtained from low-temperature pyrolysis of lignite. One important factor for low-temperature oxidation reactivity was the concentration of active sites in coal and chars. The release of volatile matter and decomposition of solid oxygenated complexes play an important role in the generation of active sites.[6] It has been reported that the possible reaction sites are free carbon centers in aromatic and aliphatic structures of coal and char, such as aliphatic C−H and benzylic CH_2.[7,39,41] The changes in the chemical structure of coal and char samples during low-temperature oxidation are discussed in the following sections.

3.4. Chemical Structure Changes during Non-isothermal Oxidation. Figure 9 shows the infrared spectra of raw coal and char samples before and after oxidation. The most remarkable changes occurred in the regions of 3700−3000 cm^{-1} (OH), 3000−2800 cm^{-1} (aliphatic C−H), and 1800−1000 cm^{-1} (C═O, COOH, C═C, and C−O). It has been postulated that the peroxygen (−OO−) is first formed when oxygen attacks the radical sites on coal, followed by the formation of hydroperoxy (−O−OH). The decomposition of hydroperoxy results in the formation of more active sites as well as carbonyl (−C═O) and carboxyl (−COOH) groups.[7,8,39,41] With increasing temperature, the rate of decomposition increases and gaseous products (CO and CO_2) are formed. To further investigate the changes in the chemical structure of coal and chars

dx.doi.org/10.1021/ef501004t | Energy Fuels 2014, 28, 5612−5622

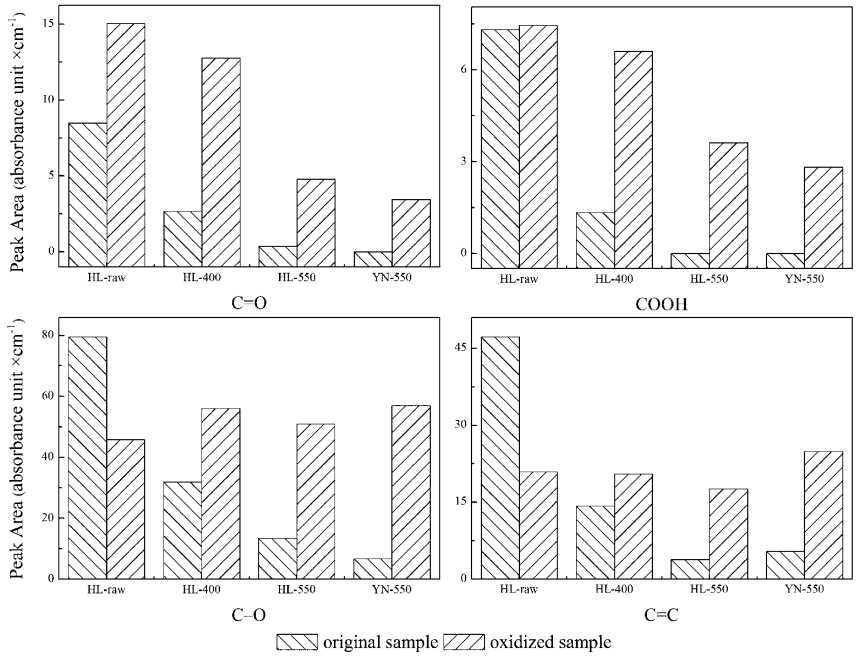

Figure 11. Changes in aromatic C═C, carbonyl, carboxyl, and C−O group adsorption during non-isothermal oxidation of coal and char samples.

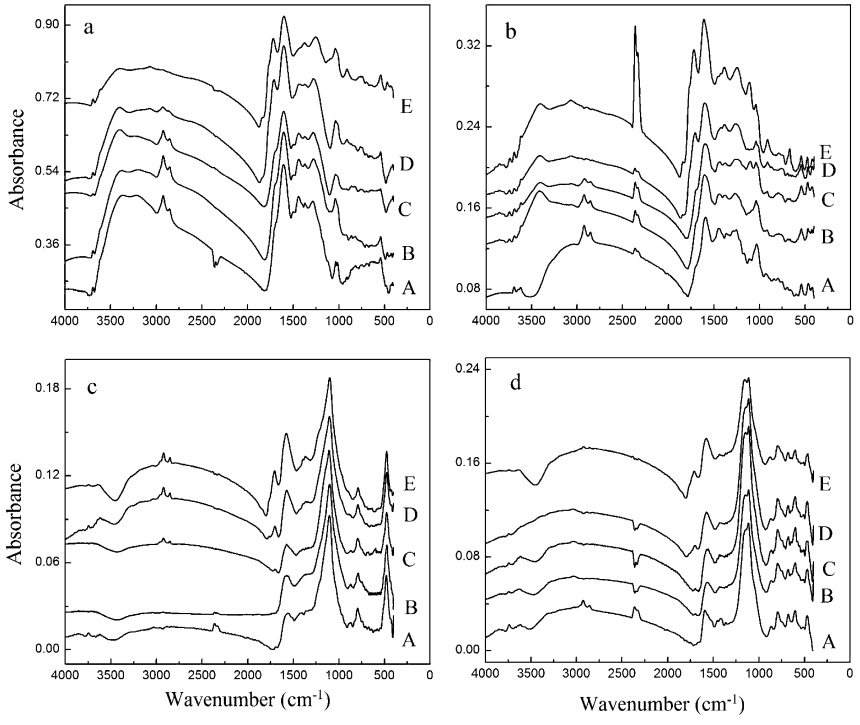

Figure 12. FTIR spectra of (A) raw coal or char samples in comparison to samples after isothermal oxidation at different temperatures for 8 h at (B) 50 °C, (C) 150 °C, (D) 250 °C, and (E) 300 °C: (a) HL raw coal, (b) HL char at 400 °C, (c) HL char at 550 °C, and (d) YN char at 550 °C.

during oxidation, the selected zones of the IR spectra were studied by curve-fitting analysis. The band positions and assignments in the FTIR spectra of the samples are listed in Table 2.

The changes in the intensities of functional groups in coal and chars after non-isothermal oxidation are shown in Figures 10 and 11. The difference in the concentrations of oxygen-containing functional groups caused by oxidation is the results of the balance between additional functional groups created by chemisorption of oxygen forming oxygen-containing functional groups and the disappearance of functional groups because of the decomposition of these groups and oxidation products. The changes in hydrogen bonds formed by OH groups of oxidized coal and char samples (Figure 10) indicated that the concentration of OH groups increased for char samples but decreased for HL raw coal. The release of volatile matter during oxidation could produce more active sites to accelerate oxidation reactions. It is clearly seen in Figure 3 that the weight loss and heat generation for HL

dx.doi.org/10.1021/ef501004t | *Energy Fuels* 2014, 28, 5612−5622

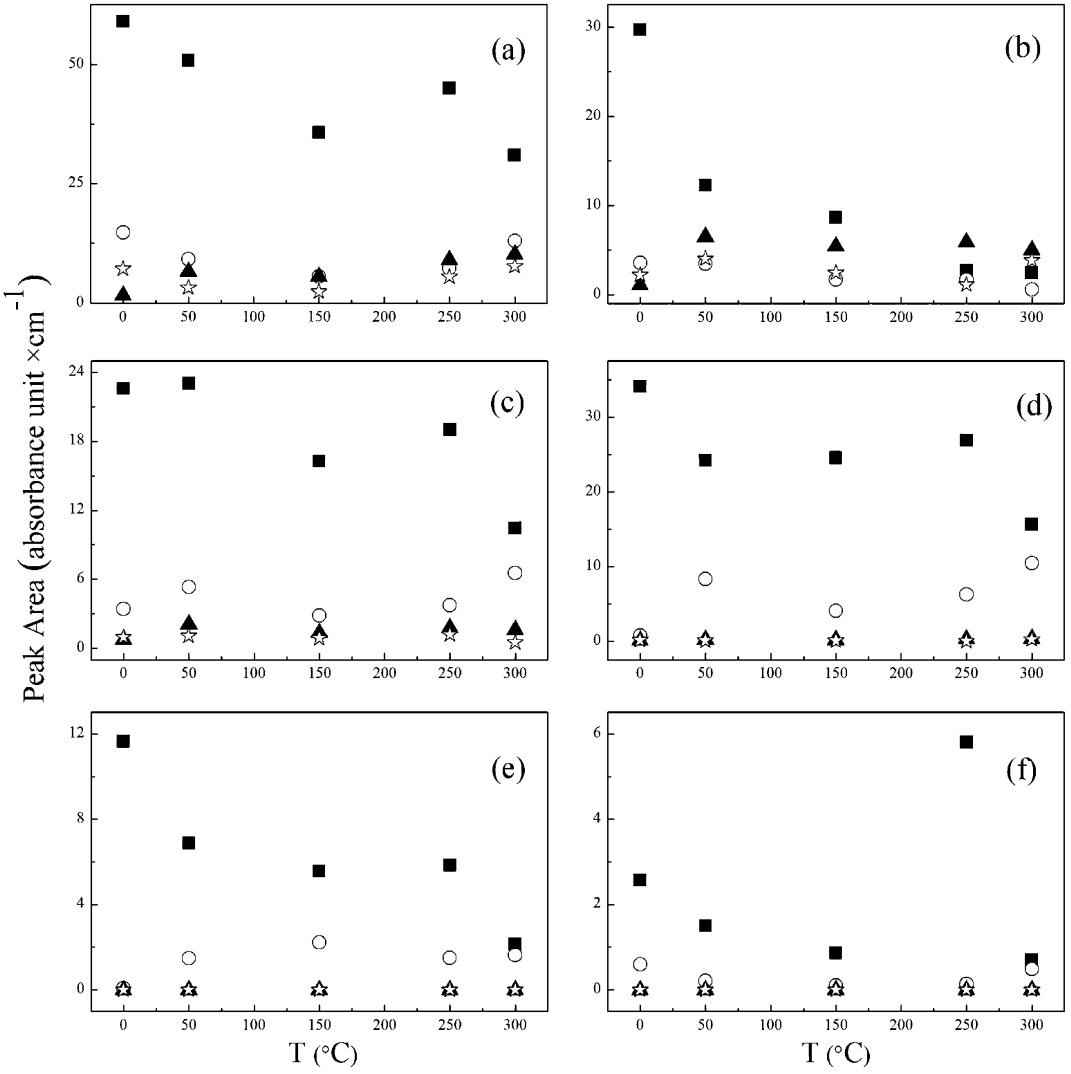

Figure 13. Changes in OH group adsorption as a function of oxidation for (a) aromatic hydrogen, (b) tightly bound cyclic OH tetramers, (c) OH−ether O hydrogen bonds, (d) self-associated OH, (e) OH−π hydrogen bonds, and (f) free OH groups: (■) HL raw coal, (○) HL char at 400 °C, (▲) HL char at 550 °C, and (☆) YN char at 550 °C.

raw coal were greater than that for char samples. The decomposition of OH groups results in the formation of water during oxidation.

The intensity of aromatic hydrogen increased in all oxidized samples compared to original samples (Figure 10). This can be attributed to the reaction between aliphatic hydrogen groups and oxygen during low-temperature oxidation. Aliphatic hydrogen groups are the first sites attacked by oxygen.[31] Aliphatic groups are less stable compared to aromatics during low-temperature oxidation and, therefore, were preferentially attacked by oxygen.[8,12,31] Other oxygen-containing groups (C═O, COOH, and C−O) also increased during oxidation (Figure 11). Figure 6 showed that the evolution of CO and CO_2 increased substantially above 180 °C during oxidation, which can be attributed to the decomposition of carboxyl and carbonyl groups.[6−8,41] The intensity of C═C vibrations followed the same trend as aromatic hydrogen for chars. However, the intensity of C═C decreased after oxidation (Figure 11) in the case of HL raw coal. Wang et al.[12] reported that C═C absorption increased at the early stages of oxidation but decreased with increasing the oxidation time, indicating that the aromatic structures decompose at later stages of oxidation. Therefore, our study is consistent with the literature.

3.5. Chemical Structure Changes during Isothermal Oxidation. Figure 12 shows the FTIR spectra of raw coal and chars in comparison to samples oxidized at 50, 150, 250, and 300 °C for 8 h. Considerable changes took place for oxygen-containing groups. For HL raw coal and char from pyrolysis at 400 °C, changes were observed in the 3700−3000 cm^{-1} region. These changes were inconspicuous in the char from pyrolysis at 550 °C. The largest peak in OH groups occurred at 3400 cm^{-1}, corresponding to self-associated OH groups (panels a and b of Figure 12), indicating that the self-associated OH groups account for the largest proportion of the 3700−3000 cm^{-1} zone during low-temperature oxidation. The reactions involving OH groups result in the formation of water. The changes in hydrogen bonds formed by OH group adsorption as a function of the oxidation temperature are shown in Figure 13. The decrease in the concentration of OH groups at temperatures above 150 °C can be attributed to the evaporation of water. At above 250 °C, the concentration of OH groups in HL raw coal increased, indicating the acceleration of the oxidation process. Above 300 °C, the concentration of OH groups in HL raw coal decreased significantly, because of the decomposition of oxygen functionalities at high

dx.doi.org/10.1021/ef501004t | *Energy Fuels* 2014, 28, 5612−5622

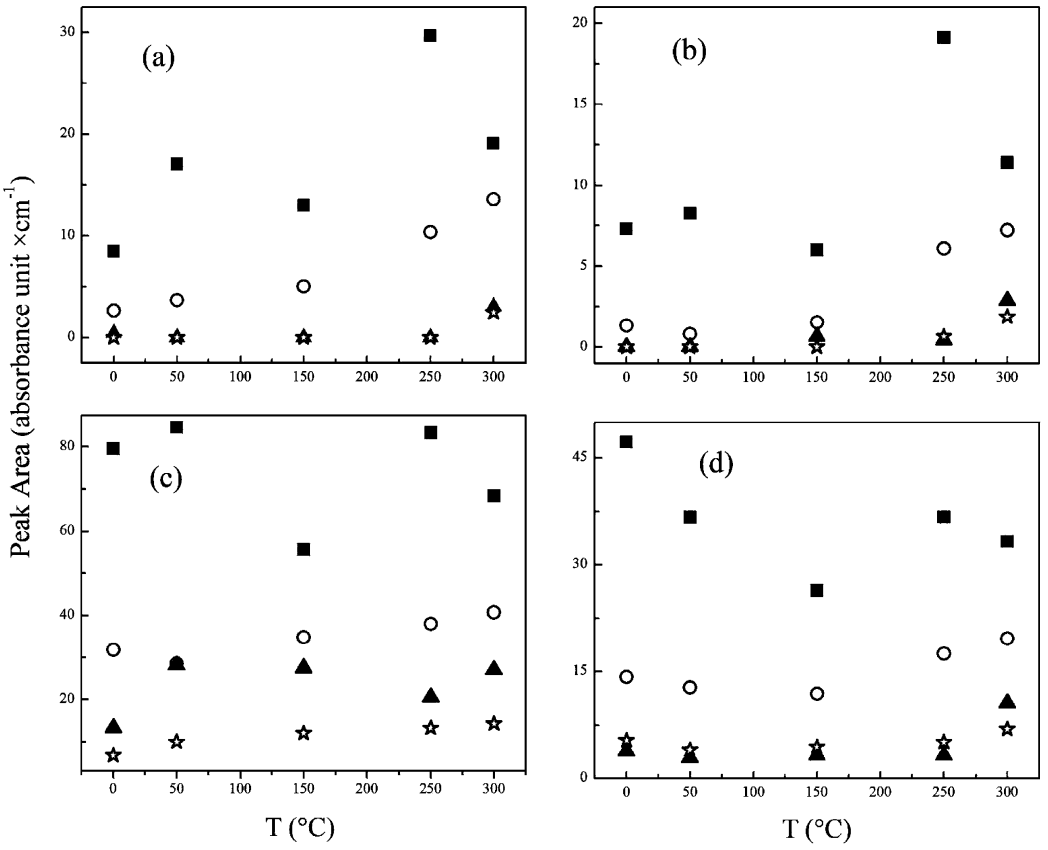

Figure 14. Changes in (a) carbonyl, (b) carboxyl, (c) C−O group, and (d) aromatic C═C of coal and char samples as a function of the oxidation temperature: (■) HL raw coal, (○) HL char at 400 °C, (▲) HL char at 550 °C, and (☆) YN char at 550 °C.

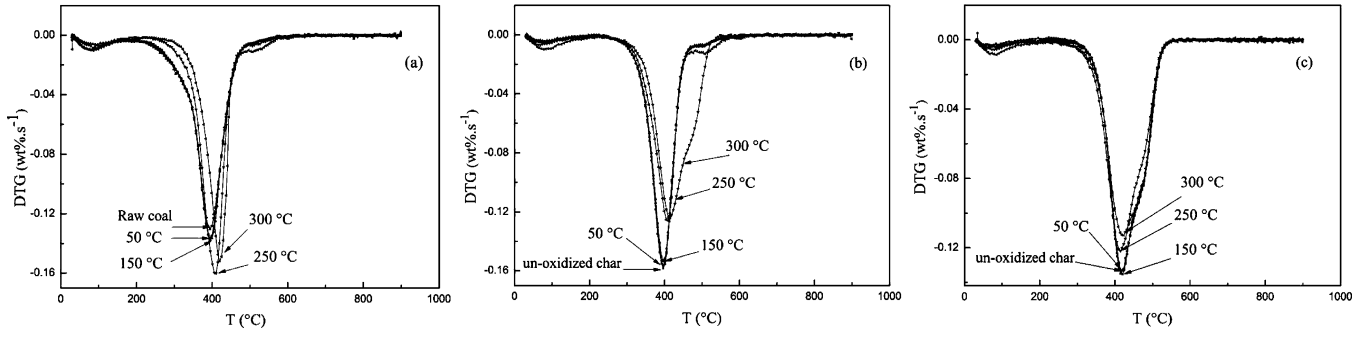

Figure 15. DTG curves of raw coal and samples oxidized at 50, 150, 250, and 300 °C for 8 h: (a) HL raw coal and its oxidized samples, (b) HL char at 550 °C and its oxidized samples, and (c) YN char at 550 °C and its oxidized samples.

temperatures. Similar trends were observed for carbonyl, carboxyl, C−O, and aromatic C═C groups (Figure 14). However, different results were observed with char samples. Unlike raw coal, the concentration of OH groups and other oxygen-containing groups in chars increased with increasing the temperature above 150 °C. This suggested that the rate of chemisorption of oxygen was greater than the decomposition of oxidation products. Therefore, chars had lower reactivity during low-temperature oxidation compared to their parent coals.

3.6. Effects of Oxidation on Combustion Reactivity. The differential thermogravimetry (DTG) curves of coal and chars before and after oxidation at 50, 150, 250, and 300 °C for 8 h are given in Figure 15. The DTG curves showed that the maximum reaction rates of oxidized HL coal were greater than that of the raw coal (Figure 15a). The opposite trend was observed in HL char and YN char from pyrolysis of coal at 550 °C (panels b and c of Figure 15). When char samples were oxidized at higher temperatures, the concentration of oxygen functionalities increased as a result of intensive oxidation (Figures 13 and 14). The increase in the concentration of oxygen complexes was accompanied by a decrease in the concentration of aliphatic structures, which are the first sites attached by oxygen during combustion. This, in turn, decreased the combustion reactivity of chars oxidized at high temperatures. Khan[5] also reported that hydrogen contents of char correlates well with its reactivity. The higher maximum reaction rates in the unoxidized HL char sample compared to raw coal can be related to the higher surface area and porosity of char compared to raw coal (Figure 4). The temperature corresponding to the maximum reaction rates (DTG_{max}) of oxidized samples was higher than those of original

dx.doi.org/10.1021/ef501004t | *Energy Fuels* 2014, 28, 5612−5622

samples. In other words, the combustion reaction was shifted to higher temperatures in oxidized samples. This can be attributed to the formation of stable oxygen complexes during low-temperature oxidation, which decompose at higher temperatures, causing an increase in the temperature corresponding to DTG_{max}.[5]

4. CONCLUSION

(1) During low-temperature oxidation, the temperature of the coal and char samples increased progressively to above the furnace temperature, i.e., above the crossing point because of the exothermic oxidation reactions. Chars prepared at 400 °C had the lowest CPT, indicating the highest oxidation reactivity at a low temperature. (2) With increasing the oxidation temperature to above 150 °C, the evolution of CO_2 and CO increased significantly for both coals. The rate of CO_2 generation significantly exceeded that of CO during oxidation of all samples. The molar ratio of CO_2/CO was around 4.15 under the present experimental conditions. (3) Isothermal oxidation experiments showed that the oxygen functional groups in raw coal decreased with increasing the oxidation temperature above 250 °C, suggesting that the rate of decomposition of oxidation products was greater than oxygen chemisorption. The opposite trend was observed for char samples. (4) The combustion reactivity of char samples decreased after their oxidation at higher temperatures.

AUTHOR INFORMATION

Corresponding Author

*Telephone: +61-2-40333902. E-mail: jianglong.yu@newcastle.edu.au.

Notes

The authors declare no competing financial interest.

ACKNOWLEDGMENTS

This study was supported by the Natural Science Foundation of China (21176109, U1361120, and 21210102058). The authors also acknowledge the financial support through the Liaoning Outstanding Professorship Program (2011).

REFERENCES

(1) Yu, J.; Tahmasebi, A.; Han, Y.; Yin, F.; Li, X. A review on water in low rank coals: The existence, interaction with coal structure and effects on coal utilization. *Fuel Process. Technol.* **2013**, *106*, 9−20.

(2) Lu, C.; Zheng, Y. M.; Yu, M. G. Research on low-temperature oxidation and pyrolysis of coal by thermal analysis experiment. *Procedia Earth Planet. Sci.* **2009**, *1*, 718−723.

(3) Qi, X.; Wang, D.; Zhong, X.; Xu, Y. Oxygen consumption of coal at low temperatures. *Procedia Earth Planet. Sci.* **2009**, *1*, 366−370.

(4) Clemens, A. H.; Matheson, T. W. The role of moisture in the self-heating of low-rank coals. *Fuel* **1996**, *75*, 891−895.

(5) Khan, M. R. Significance of char active surface area for appraising the reactivity of low- and high-temperature chars. *Fuel* **1987**, *66*, 1626−1634.

(6) Wang, H.; Dlugogorski, B. Z.; Kennedy, E. M. Thermal decomposition of solid oxygenated complexes formed by coal oxidation at low temperatures. *Fuel* **2002**, *81*, 1913−1923.

(7) Wang, H.; Dlugogorski, B. Z.; Kennedy, E. M. Analysis of the mechanism of the low-temperature oxidation of coal. *Combust. Flame* **2003**, *134*, 107−117.

(8) Yürüm, Y.; Altuntaş, N. Air oxidation of Beypazari lignite at 50 °C, 100 °C and 150 °C. *Fuel* **1998**, *77*, 1809−1814.

(9) Jakab, E.; Till, F.; Várhegyi, G. Thermogravimetric-mass spectrometric study on the low temperature oxidation of coals. *Fuel Process. Technol.* **1991**, *28*, 221−238.

(10) Wang, D.; Zhong, X.; Gu, J.; Qi, X. Changes in active functional groups during low-temperature oxidation of coal. *Min. Sci. Technol. (Xuzhou, China)* **2010**, *20*, 35−40.

(11) Shamsi, A.; Shadle, L. J.; Seshadri, K. S. Study of low-temperature oxidation of buckskin subbituminous coal and derived chars produced in ENCOAL process. *Fuel Process. Technol.* **2004**, *86*, 275−292.

(12) Wang, G.; Zhou, A. Time evolution of coal structure during low temperature air oxidation. *Int. J. Min. Sci. Technol.* **2012**, *22*, 517−521.

(13) Koch, A.; Krzton, A.; Finqueneisel, G.; Heintz, O.; Weber, J.; Zimny, T. A study of carbonaceous char oxidation in air by semi-quantitative FTIR spectroscopy. *Fuel* **1998**, *77*, 563−569.

(14) Skodras, G.; Natas, P.; Basinas, P.; Sakellaropoulos, G. P. Effects of pyrolysis temperature, residence time on the reactivity of clean coals produced from poor quality coals. *Global NEST J.* **2006**, *8*, 89−94.

(15) Roberts, R. M.; Sweeney, K. M. Low-temperature pyrolysis of Texas lignite, basic extracts and some related model compounds. *Fuel* **1984**, *63*, 904−908.

(16) Meng, F.; Yu, J.; Tahmasebi, A.; Han, Y.; Zhao, H.; Lucas, J.; Wall, T. Characteristics of chars from low-temperature pyrolysis of lignite. *Energy Fuels* **2014**, *28*, 275−284.

(17) Haykiri-Acma, H.; Yaman, S.; Kucukbayrak, S. Effect of pyrolysis temperature on burning reactivity of lignite char. *Energy Educ. Sci. Technol., Part A* **2012**, *29*, 1203−1216.

(18) Wang, H.; Dlugogorski, B. Z.; Kennedy, E. M. Experimental study on low-temperature oxidation of an Australian coal. *Energy Fuels* **1999**, *13*, 1173−1179.

(19) Choi, H.; Thiruppathiraja, C.; Kim, S.; Rhim, Y.; Lim, J.; Lee, S. Moisture readsorption and low temperature oxidation characteristics of upgraded low rank coal. *Fuel Process. Technol.* **2011**, *92*, 2005−2010.

(20) Küçük, A.; Kadıoğlu, Y.; Gülaboğlu, M. Ş. A study of spontaneous combustion characteristics of a turkish lignite: Particle size, moisture of coal, humidity of air. *Combust. Flame* **2003**, *133*, 255−261.

(21) Feng, B.; Bhatia, S. K. Variation of the pore structure of coal chars during gasification. *Carbon* **2003**, *41*, 507−523.

(22) Radović, L. R.; Walker, P. L., Jr.; Jenkins, R. G. Importance of carbon active sites in the gasification of coal chars. *Fuel* **1983**, *62*, 849−856.

(23) Fei, H.; Hu, S.; Xiang, J.; Sun, L.; Fu, P.; Chen, G. Study on coal chars combustion under O_2/CO_2 atmosphere with fractal random pore model. *Fuel* **2011**, *90*, 441−448.

(24) Painter, P. C.; Sobkowiak, M.; Youtcheff, J. FTIR study of hydrogen bonding in coal. *Fuel* **1987**, *66*, 973−978.

(25) Solomon, P. R.; Carangelo, R. M. FTIR analysis of coal: 2. Aliphatic and aromatic hydrogen concentration. *Fuel* **1988**, *67*, 949−959.

(26) Ibarra, J.; Moliner, R.; Gavilán, M. P. Functional group dependence of cross-linking reactions during pyrolysis of coal. *Fuel* **1991**, *70*, 408−413.

(27) Tahmasebi, A.; Yu, J.; Han, Y.; Yin, F.; Bhattacharya, S.; Stokie, D. Study of chemical structure changes of Chinese lignite upon drying in superheated steam, microwave, and hot air. *Energy Fuels* **2012**, *26*, 3651−3660.

(28) Tahmasebi, A.; Yu, J.; Bhattacharya, S. Chemical structure changes accompanying fluidized-bed drying of Victorian brown coals in superheated steam, nitrogen, and hot air. *Energy Fuels* **2012**, *27*, 154−166.

(29) Taulbee, D. N.; Sparks, J.; Robl, T. L. Application of hot stage micro-FTIR to the study of organic functional group changes during pyrolysis. *Fuel* **1994**, *73*, 1551−1556.

(30) Ibarra, J.; Muñoz, E.; Moliner, R. FTIR study of the evolution of coal structure during the coalification process. *Org. Geochem.* **1996**, *24*, 725−735.

(31) Tahmasebi, A.; Yu, J.; Han, Y.; Li, X. A study of chemical structure changes of Chinese lignite during fluidized-bed drying in nitrogen and air. *Fuel Process. Technol.* **2012**, *101*, 85−93.

(32) Ibarra, J.; Moliner, R.; Bonet, A. J. FTIR investigation on char formation during the early stages of coal pyrolysis. *Fuel* **1994**, *73*, 918−924.

(33) Miura, K.; Mae, K.; Li, W.; Kusakawa, T.; Morozumi, F.; Kumano, A. Estimation of hydrogen bond distribution in coal through the analysis of OH stretching bands in diffuse reflectance infrared spectrum measured by in-situ technique. *Energy Fuels* **2001**, *15*, 599−610.
(34) Miura, K.; Mae, K.; Morozumi, F. A new method estimate hydrogen bondings in coal by utilizing FTIR and DSC. *Prepr. Pap.—Am. Chem. Soc., Div. Fuel Chem.* **1997**, *42*, 209−213.
(35) Painter, P. C.; Coleman, M. M.; Jenkins, R. G.; Whang, P. W.; Walker, P. L., Jr. Fourier transform infrared study of mineral matter in coal. A novel method for quantitative mineralogical analysis. *Fuel* **1978**, *57*, 337−344.
(36) Painter, P. C.; Snyder, R. W.; Youtcheff, J.; Given, P. H.; Gong, H.; Suhr, N. Analysis of kaolinite in coal by infrared spectroscopy. *Fuel* **1980**, *59*, 364−366.
(37) Finkelman, R. B.; Fiene, F. L.; Painter, P. C. Determination of kaolinite in coal by infrared spectroscopy—A comment. *Fuel* **1981**, *60*, 643−644.
(38) Wang, H.; Dlugogorski, B. Z.; Kennedy, E. M. Examination of CO_2, CO, and H_2O formation during low-temperature oxidation of a bituminous coal. *Energy Fuels* **2002**, *16*, 586−592.
(39) Wang, H.; Dlugogorski, B. Z.; Kennedy, E. M. Coal oxidation at low temperatures: Oxygen consumption, oxidation products, reaction mechanism and kinetic modelling. *Prog. Energy Combust. Sci.* **2003**, *29*, 487−513.
(40) Krishnaswamy, S.; Gunn, R. D.; Agarwal, P. K. Low-temperature oxidation of coal. 2. An experimental and modelling investigation using a fixed-bed isothermal flow reactor. *Fuel* **1996**, *75*, 344−352.
(41) Clemens, A. H.; Matheson, T. W.; Rogers, D. E. Low temperature oxidation studies of dried New Zealand coals. *Fuel* **1991**, *70*, 215−221.